

Effects of landscape modification on coastal sediment nitrogen availability, microbial functional gene abundances and N₂O production potential across the tropical-subtropical gradient

Article

Accepted Version

Yang, P., Tang, K. W., Zhang, L., Lin, X., Yang, H. ORCID: <https://orcid.org/0000-0001-9940-8273>, Tong, C., Hong, Y., Tan, L., Lai, D. Y. F., Tian, Y., Zhu, W., Ruan, M. and Lin, Y. (2023) Effects of landscape modification on coastal sediment nitrogen availability, microbial functional gene abundances and N₂O production potential across the tropical-subtropical gradient. *Environmental research*, 227. 115829. ISSN 1096-0953 doi: <https://doi.org/10.1016/j.envres.2023.115829> Available at <https://centaur.reading.ac.uk/111615/>

It is advisable to refer to the publisher's version if you intend to cite from the work. See [Guidance on citing](#).

To link to this article DOI: <http://dx.doi.org/10.1016/j.envres.2023.115829>

Publisher: Elsevier

including copyright law. Copyright and IPR is retained by the creators or other copyright holders. Terms and conditions for use of this material are defined in the [End User Agreement](#).

www.reading.ac.uk/centaur

CentAUR

Central Archive at the University of Reading

Reading's research outputs online

Effects of landscape modification on coastal sediment nitrogen availability, microbial functional gene abundances and N₂O production potential across the tropical-subtropical gradient

Ping Yang^{a,b,c,d}, Kam Tang^e, Linhai Zhang^{a,b}, Xiao Lin^{a,b,c}, Hong Yang^{f,g}, Chuan Tong^{a,b,d}, Yan Hong^a, Lishan Tan^h, Derrick .F. Lai^h, Yalan Tian^a, Wanyi Zhu^a, Manjing Ruan^a, Yongxin Lin^{a b c}

a School of Geographical Sciences, Fujian Normal University, Fuzhou, 350117, PR China

b Institute of Geography, Fujian Normal University, Fuzhou, 350117, PR China

c Fujian Provincial Key Laboratory for Subtropical Resources and Environment, Fujian Normal University, Fuzhou, 350117, PR China

d Key Laboratory of Humid Subtropical Eco-geographical Process of Ministry of Education, Fujian Normal University, Fuzhou, 350117, PR China

e Department of Biosciences, Swansea University, Swansea, SA2 8PP, UK

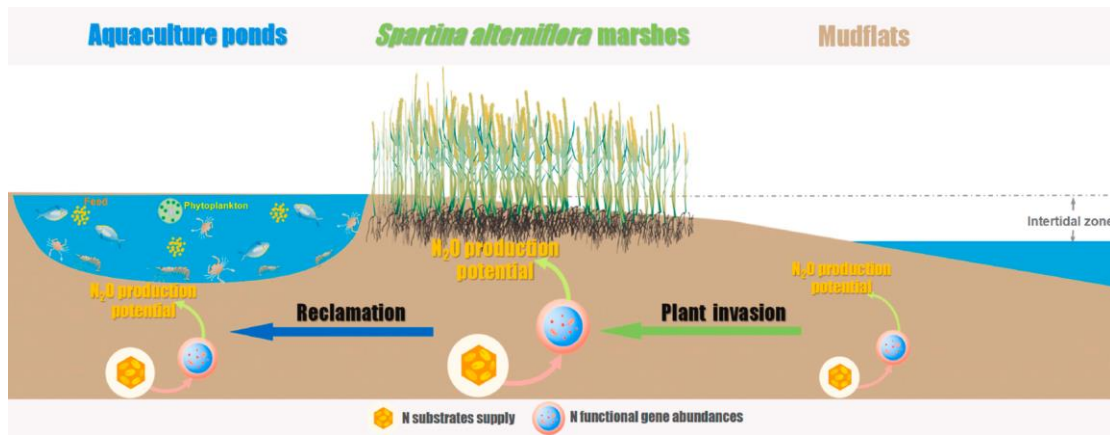
f College of Environmental Science and Engineering, Fujian Normal University, Fuzhou, 350007, China

g Department of Geography and Environmental Science, University of Reading, Reading, RG6 6AB, UK

h Department of Geography and Resource Management, The Chinese University of Hong Kong, Shatin, New Territories, Hong Kong SAR, China

Abstract

Wetland sediment is an important nitrogen pool and a source of the greenhouse gas nitrous oxide (N₂O). Modification of coastal wetland landscape due to plant invasion and aquaculture activities may drastically change this N pool and the related dynamics of N₂O. This study measured the sediment properties, N₂O production and relevant functional gene abundances in 21 coastal wetlands across five provinces along the tropical-subtropical gradient in China, which all had experienced the same sequence of habitat transformation from native mudflats (MFs) to invasive *Spartina alterniflora* marshes (SAs) and subsequently to aquaculture ponds (APs). Our results showed that change from MFs to SAs increased the availability of NH₄⁺-N and NO₃⁻-N and the abundance of functional genes related to N₂O production (*amoA*, *nirK*, *nosZ* I, and *nosZ* II), whereas conversion of SAs to APs resulted in the opposite changes. Invasion of MFs by *S. alterniflora* increased N₂O production potential by 127.9%, whereas converting SAs to APs decreased it by 30.4%. Based on structural equation modelling, nitrogen substrate availability and abundance of ammonia oxidizers were the key factors driving the change in sediment N₂O production potential in these wetlands. This study revealed the main effect patterns of habitat modification on sediment biogeochemistry and N₂O production across a broad geographical and climate gradient. These findings will help large-scale mapping and assessing landscape change effects on sediment properties and greenhouse gas emissions along the coast.



1. Introduction

The atmospheric concentration of the powerful greenhouse gas nitrous oxide (N_2O) has increased by 123% since the beginning of the industrial era, reaching 333.2 ppbv in 2020 (World Meteorological Organization, 2021). A major source of terrestrial N_2O is microbial transformation of nitrogen (IPCC, 2019) via both nitrification and denitrification (Butterbach-Bahl et al., 2013; Gao et al., 2021; Toyoda et al., 2011; Wu et al., 2019). Quantifying the nitrogen substrate pool, the relevant microbial communities and their activities would be key to understanding N_2O dynamics globally.

Despite covering just 8% of the global land area, wetlands represent one of the world's largest terrestrial nitrogen inventories (Batjes, 1996; Xu et al., 2020). Coastal wetlands are particularly important for nitrogen storage (Batjes, 1996; Yang et al., 2016) owing to their high rates of sedimentation and organic matter burial (Chmura et al., 2003; He et al., 2021). Unfortunately, coastal wetlands are increasingly subject to habitat degradation and modification due to land-use change and exotic plant invasion (Murray et al., 2019; Sun et al., 2015; Walker and Smith, 1992), which would likely alter the sediment properties and related microbial production of greenhouse gases such as N_2O (Bahram et al., 2022; Tan et al., 2022; Tian et al., 2020).

There is a total of 5.79×10^6 ha of coastal wetlands along the southern and eastern seaboard of mainland China, accounting for about 10% of the total natural wetlands in the country (Sun et al., 2015). There have been small-scale studies on the effects of habitat change (e.g., plant invasion, agroforestry reclamations, aquaculture reclamation, etc.) on nitrogen mineralization and N_2O emissions in these coastal wetlands (Gao et al., 2019a, 2019b; He et al., 2021; Tan et al., 2020; Yang et al., 2016, 2017; Zhang et al., 2016). In the recent decades, many coastal areas in China have undergone similar sequence of landscape change, with mudflats transformed by the invasion of the exotic cordgrass *Spartina alterniflora* and subsequent clearing of the marsh to construct aquaculture ponds (Duan et al., 2020; Sun et al., 2015; Ren et al., 2019). This provides an opportunity to examine the general pattern of landscape modification effects on sediment properties and N_2O production across the broad geographical range.

Ideally, a proper assessment of the landscape change effects would require comparing the habitat characteristics and N_2O production before and after modification. However, such time-lapsed study is not possible because many of the impacted coastal areas in China lack historical information and routine monitoring. Instead, we took samples from 21 coastal wetlands along a 2500-km long transect across the tropical and subtropical zones. Large areas of these wetlands have undergone the same sequence of transformation, from native non-vegetated mudflats to *S. alterniflora* marshes and subsequently to aquaculture ponds. By analyzing the sediments' physicochemical properties, nitrogen-cycling functional gene abundances and N_2O production potentials in all three habitat types, we were able to derive

common effect patterns of habitat modifications on sediment N₂O production, regardless of differences in local climate, habitat age, environmental conditions and aquaculture practices. This knowledge will be essential for assessing landscape change effects on greenhouse gas budget at the regional to national scale.

This study hypothesized that the conversion of mudflats to *S. alterniflora* marshes would increase the abundances of nitrogen-cycling functional genes and N₂O production potential in the sediment, thanks to an increased supply of nitrogen substrates by the vegetation. Conversely, this study hypothesized that removal of *S. alterniflora* from aquaculture ponds and routine management of pond sediment would decrease nitrogen substrate supply to the sediment, disrupt the sediment microbial community and lower the N₂O production potential.

2. Materials and methods

2.1. Study area and sample collection

Sediment samples were collected at 21 coastal wetland sites across the tropical and subtropical climate zones in southeastern China (20°42' N to 31°51' N; 109°11' E to 122°11' E) (Fig. 1). These sites span five provinces, with two sites in Shanghai (SH), six in Zhejiang (ZJ), nine in Fujian (FJ), three in Guangdong (GD) and one in Guangxi (GX) (Fig. 1). The annual average temperature varied from 11.0 to 23.0 °C and precipitation from 100 to 220 cm across the five provinces. Coastal wetlands in these five provinces cover an area of 2.58×10^6 ha, accounting for 44.5% of the total area of coastal wetlands in China (Sun et al., 2015). There was approximately 3.6×10^5 ha of tidal flats along the coastal zone of the five provinces (Jia et al., 2021), representing 42.4% of the total areas of tidal flats in China. Many of these coastal wetlands have been impacted by the invasion of *S. alterniflora* and subsequent conversion to aquaculture ponds. Along these coastal zones, *S. alterniflora* marshes cover an area of 3.34×10^4 ha which account for 61.2% of the total *Spartina* marsh area in China (Liu et al., 2018), whereas the aquaculture ponds cover an area of 5.31×10^5 ha, equivalent to 36.9% of the total aquaculture pond area in the country (Duan et al., 2020).



Fig. 1. Locations of the 21 coastal wetland sites in southeastern China. At each site, three habitat types were sampled, including mudflats, *Spartina alterniflora* marshes and aquaculture ponds.

Field sampling campaigns were carried out in the three habitat types at each of the 21 coastal wetland sites, namely native mudflats (MFs), *S. alterniflora* marshes (SAs) and aquaculture ponds (APs), between December 2019 and January 2020. One surface (top 20 cm) sediment

sample from each of the triplicate plots established in each habitat was collected with a steel corer (5 cm internal diameter), for a total of 189 surface sediment samples. All sediment samples were kept at 4 °C until use (Hellman et al., 2019).

2.2. Determination of sediment physicochemical properties

In the laboratory, each sediment sample was sifted through a 2-mm sieve before the analysis of various physicochemical parameters. Sediment pH and salinity were measured with a pH meter (Orion 868, USA; a 1:2.5 v/v sediment-deionized water mixture) and a salinity meter (Salt6, Eutech Instruments, USA; a 1:5 v/v sediment-deionized water mixture), respectively. Sediment particle size was measured with a laser particle size analyzer (Master Sizer 2000; Malvern Scientific Instruments, Suffolk, UK). Sediment NO_3^- -N and NH_4^+ -N were extracted with 2 M KCl solution (Gao et al., 2019b; Yin et al., 2017) and the concentrations of NO_3^- -N and NH_4^+ -N in the extracts were measured with a flow injection analyzer (Skalar Analytical SAN++, Netherlands). Sediment microbial biomass nitrogen (MBN) content was determined by the fumigation-extraction method (Templer et al., 2003). The concentrations of SO_4^{2-} and Cl^- in sediments were measured with an ion chromatograph (Dionex 2100, USA) following the methods of Chen and Sun (2020).

2.3. DNA extraction and real-time quantitative PCR

Genomic DNA was extracted from each 0.5 g of freeze-dried sediment using FastDNA Spin Kit for Soil (MP Biomedicals, CA, USA) according to the manufacturer's protocol. The quality and quantity of extracted DNA was verified by gel electrophoresis and spectrophotometry (NanoDrop Technologies, Wilmington, USA).

Quantification of nitrogen-cycling functional genes was performed using a real-time polymerase chain reaction (PCR) detection system (CFX384, Bio-Rad Laboratories Inc., Hercules, CA, USA). Each reaction mixture (10 μL) contained 5 μL SYBR mix, an optimized concentration of forward and reverse primers, 1 μL of template (containing approximately 1–10 ng of DNA) and sterilized distilled water. Three negative controls with sterilized distilled water instead of DNA templates were included in the analysis. Nitrogen-cycling functional genes involved in ammonia oxidation (ammonia-oxidizing archaea (AOA) *amoA* and ammonia-oxidizing bacteria (AOB) *amoA*) and denitrification (*nirK*, *nirS*, *nosZ* I, and *nosZ* II) were determined and the details of primers and thermal cycling conditions for PCR are shown in Table S1. The specificity of PCR amplification was assessed by gel electrophoresis and melt curves. Standard curves were generated from a tenfold serial dilution of plasmid DNA containing the target genes. The reaction efficiency ranged from 88 to 99% with an R^2 value of 0.991–0.998.

2.4. Determination of sediment N_2O production potential

The sediment N_2O production potential was measured by anaerobic slurry incubation (Liu et al., 2019; Wang et al., 2017). While sediment N_2O production involves both oxic (e.g. nitrification) and anoxic processes (e.g. denitrification), the terminal step of the process often occurs in anoxic condition (Hu et al., 2015); therefore, we used anaerobic slurry incubation to estimate the *in situ* N_2O production potential. Approximately 30 g of each wet sediment sample and 30 mL of deoxygenated *in situ* overlying water were added to a 200 mL glass bottle and then flushed with N_2 gas (>99.9999% purity) for 5–8 min to create an anoxic condition. All bottles were then incubated for 48 h at the *in situ* temperature, and headspace gas samples were taken at 0, 24, and 48 h. Prior to gas sampling, each glass bottle was shaken on a rotary shaker at 200 rpm for 0.5 h to drive all the N_2O produced in sediment into the headspace. Subsequently, 5 mL of the headspace gas samples were taken with a syringe and 5 mL of pure N_2 gas was added back to each bottle to maintain the atmospheric pressure. The N_2O concentrations in the collected gas samples were measured on a gas chromatograph (GC-2014, Shimadzu, Japan) equipped with an electron capture detector. N_2O production potential [$\text{ng N}_2\text{O g}^{-1}$ (dry weight) day^{-1}] was then determined based on the change in cumulative N_2O produced per gram of dry sediment over time (Liu et al., 2019; Wang et al., 2017).

2.5. Statistical analysis

Significant differences in sediment physicochemical properties, nitrogen-cycling functional gene abundances, and N₂O production potential among the three habitats were tested by analysis of variance (ANOVA) using the SPSS version 25.0 (IBM, Armonk, NY, USA). Statistical plots were generated using OriginPro 2021 (OriginLab Corp. USA). Pearson correlation analysis was used to examine the relationships between sediment physicochemical properties, nitrogen-cycling functional genes abundances, and N₂O production potential using the vegan package in R software (Version 4.1.0). Structural equation modelling (SEM) was performed using AMOS 21.0 (Amos Development Corporation, Chicago, IL, USA) to evaluate the direct or indirect relationships between habitat change, sediment physicochemical properties, nitrogen-cycling functional gene abundances and N₂O production potential. *A priori* model was established based on our hypotheses and adjusted to achieve an optimal model fit based on the modification indices in the AMOS software (Bahram et al., 2022). Three commonly used indices were selected to assess the goodness of fit of the model, namely Chi-square test (χ^2), goodness of fit index (GFI) and root mean square error of approximation (RMSEA).

3. Results

3.1. Sediment physico-chemical properties

Across all 21 wetland sites, sediment NH₄⁺-N concentration (mean \pm SE) in SAs (24.0 \pm 1.3 mg kg⁻¹) was significantly higher than that in APs (16.9 \pm 1.0 mg kg⁻¹), which was in turn higher than that in MFs (13.3 \pm 0.8 mg kg⁻¹) ($p < 0.01$, Fig. 2a). NO₃⁻-N concentration in SAs (1.8 \pm 0.1 mg kg⁻¹) was higher than that in MFs (1.3 \pm 0.1 mg kg⁻¹) and APs (1.5 \pm 0.1 mg kg⁻¹) ($p < 0.01$; Fig. 2b). MBN concentration was the highest in SAs (26.6 \pm 1.9 mg kg⁻¹), followed by APs (16.8 \pm 0.8 mg kg⁻¹) and MFs (12.7 \pm 0.7 mg kg⁻¹) ($p < 0.01$; Fig. 2c). No significant differences were found in sediment pH, salinity, bulk density and percent clay particles among the three habitat types (Table S2). Mean sediment Cl⁻ concentration was significantly higher in SAs (40.9 mg kg⁻¹) than in MFs (36.8 mg kg⁻¹) and APs (37.8 mg kg⁻¹), while mean sediment SO₄²⁻ concentration was significantly higher in APs (17.5 mg kg⁻¹) than in MFs (8.9 mg kg⁻¹) and SAs (9.1 mg kg⁻¹) (Table S2).

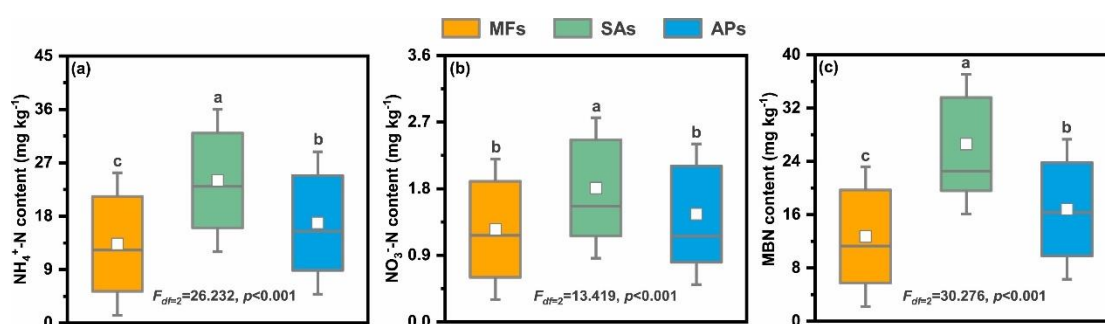


Fig. 2. Box plots of nitrogen substrates (NH₄⁺-N, NO₃⁻-N) and microbial biomass nitrogen (MBN) in surface sediment of the three wetland habitat types: mudflats (MFs), *S. alterniflora* marshes (SAs) and aquaculture ponds (APs). [The boxes, center line, and whiskers represent the 25th – 75th percentiles, median value, and 5th and 95th percentiles, respectively.] Different letters above the boxes indicate significant differences between habitat types ($p < 0.05$).

3.2. Functional gene abundances

The copy numbers of genes for ammonia oxidation (ammonia-oxidizing archaea (AOA) *amoA* and ammonia-oxidizing bacteria (AOB) *amoA*) and denitrification (*nirK*, *nirS*, *nosZ I*, and *nosZ II*) in the different habitat types are shown in Fig. 3. Overall, the

mean copy numbers of the AOA *amoA*, AOB *amoA* and *nirK* genes were significantly higher in SAs (5.46×10^6 , 2.28×10^7 and 9.89×10^7 copies g^{-1} , respectively) than in both APs (2.96×10^6 , 1.49×10^7 and 6.77×10^7 copies g^{-1} , respectively) and MFs (2.74×10^6 , 1.34×10^7 and 5.83×10^7 copies g^{-1} , respectively) ($p < 0.01$; Fig. 3a–c). The mean copy number of the *nirS* genes was significantly higher in APs (13.38×10^7 copies g^{-1}) than in both SAs (9.45×10^7 copies g^{-1}) and MFs (6.99×10^7 copies g^{-1}) ($p < 0.01$; Fig. 3d). MFs tended to have fewer copies of both *nosZ* I and *nosZ* II genes (6.57×10^7 and 9.72×10^7 copies g^{-1} , respectively) than the other habitat types ($p < 0.005$; Fig. 3e and f).

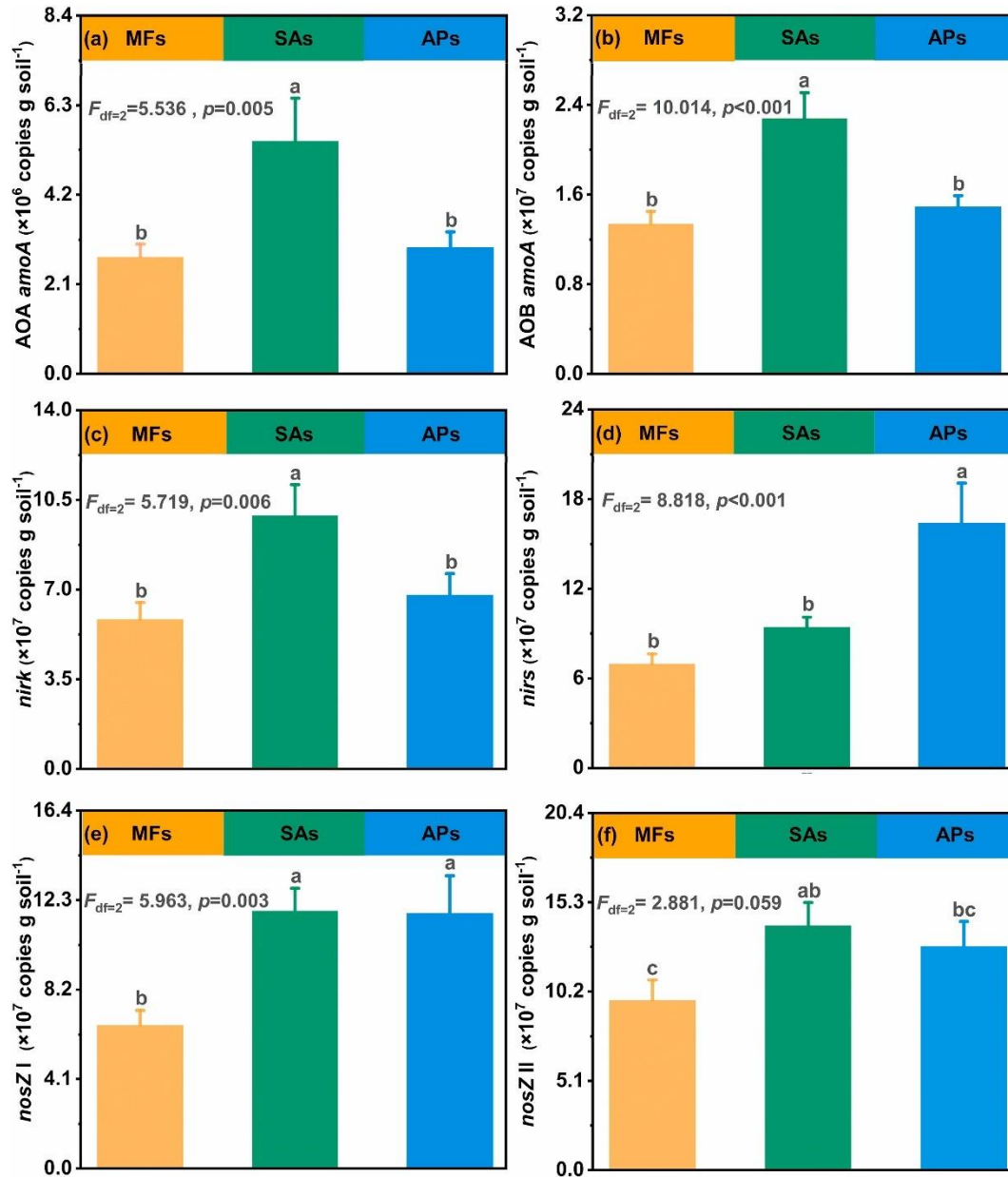


Fig. 3. Sediment gene abundances (AOA *amoA*, AOB *amoA*, *nirK*, *nirS*, *nosZ* I and *nosZ* II) in the three habitat types: mudflats (MFs), *S. alterniflora* marshes (SAs) and aquaculture ponds (APs). Bars represent mean \pm 1SE ($n = 63$). Different letters above the bars indicate significant differences ($p < 0.05$) between the habitat types.

3.3. Sediment N₂O production potential

The mean sediment N₂O production potential varied considerably between sites, ranging 30.8–176.4 ng $g^{-1} d^{-1}$ in MFs, 30.8–388.4 ng $g^{-1} d^{-1}$ in SAs, and 64.1–327.7 ng $g^{-1} d^{-1}$ in APs (Fig. 4a). Across all 21 wetland sites, the mean (\pm SE) sediment N₂O production potential was

the highest in SAs ($217.1 \pm 13.7 \text{ ng g}^{-1} \text{ d}^{-1}$), followed by APs ($151.1 \pm 9.3 \text{ ng g}^{-1} \text{ d}^{-1}$) and MFs ($95.3 \pm 9.3 \text{ ng g}^{-1} \text{ d}^{-1}$) ($p < 0.01$; Fig. 4b). Therefore, the conversion of MFs to SAs increased sediment N_2O production potential by 127.9%, while the conversion of SAs to APs decreased N_2O production potential by 30.4%.

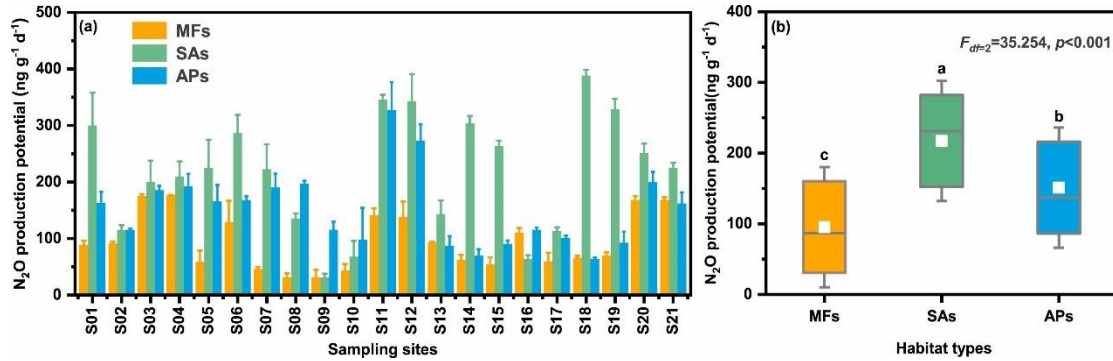


Fig. 4. (a) Sediment N_2O production potential in the three habitat types: mudflats (MFs), *S. alterniflora* marshes (SAs) and aquaculture ponds (APs) at each of the wetland sites. (b) Data from all 21 wetland sites combined in box plots to compare sediment N_2O production potentials between habitat types; different letters above the boxes indicate significant differences ($p < 0.05$).

3.4. Environmental control of sediment N_2O production potential

The results of Pearson correlation analysis between sediment N_2O production potential and various biotic and abiotic variables are shown in Fig. 5. For the conversion of MFs to SAs, sediment N_2O production potential was positively correlated to the abundances of AOA *amoA*, AOB *amoA*, *nirK*, *nirS* and *nosZ I* ($p < 0.05$), as well as the concentrations of NO_3^- -N, NH_4^+ -N and MBN ($p < 0.001$), but negatively correlated with sediment pH ($p < 0.05$; Fig. 5a). For the conversion of SAs to APs, sediment N_2O production potential was positively correlated to the abundances of AOA *amoA*, AOB *amoA* and *nirK* ($p < 0.05$) and the concentrations of NO_3^- -N, NH_4^+ -N and MBN ($p < 0.001$), but negatively correlated with sediment pH ($p < 0.001$) and *nosZ II* ($p < 0.05$; Fig. 5b). The results of SEM analysis revealed that changes in sediment N_2O production potential were mediated mainly through changes in the concentrations of NH_4^+ -N and MBN in both habitat modification scenarios (Fig. 6a and b). Overall, the concentrations of nitrogen substrates (NO_3^- -N and NH_4^+ -N) and microbial biomass (MBN) had the largest standardized positive effects on sediment N_2O production potential (Fig. 6c and d). In addition, AOA *amoA* was the most important among all functional genes in affecting sediment N_2O production potential during habitat change.

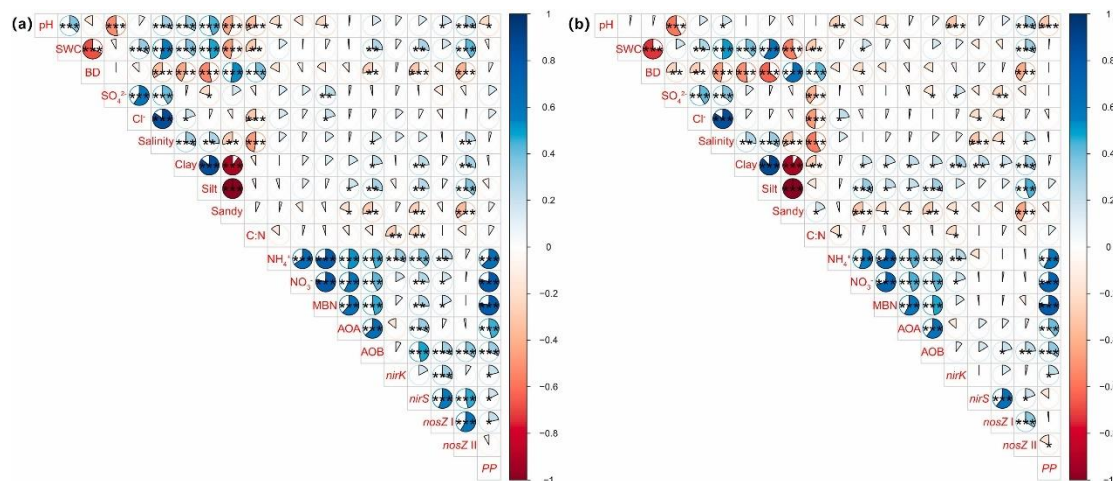


Fig. 5. Correlations among environmental variables, abundances of nitrogen-cycling functional genes and sediment N_2O production potential (PP) ($n = 216$) for the different habitat modification scenarios: (a) conversion of mudflats to *S. alterniflora* marshes; (b) conversion of *S. alterniflora* marshes to aquaculture ponds. Color of the pie indicates the direction of correlation (blue = positive; red = negative). Size of the pie is proportional to the r^2 value. Asterisks indicate levels of significance (* $p < 0.05$; ** $p < 0.01$; *** $p < 0.001$).

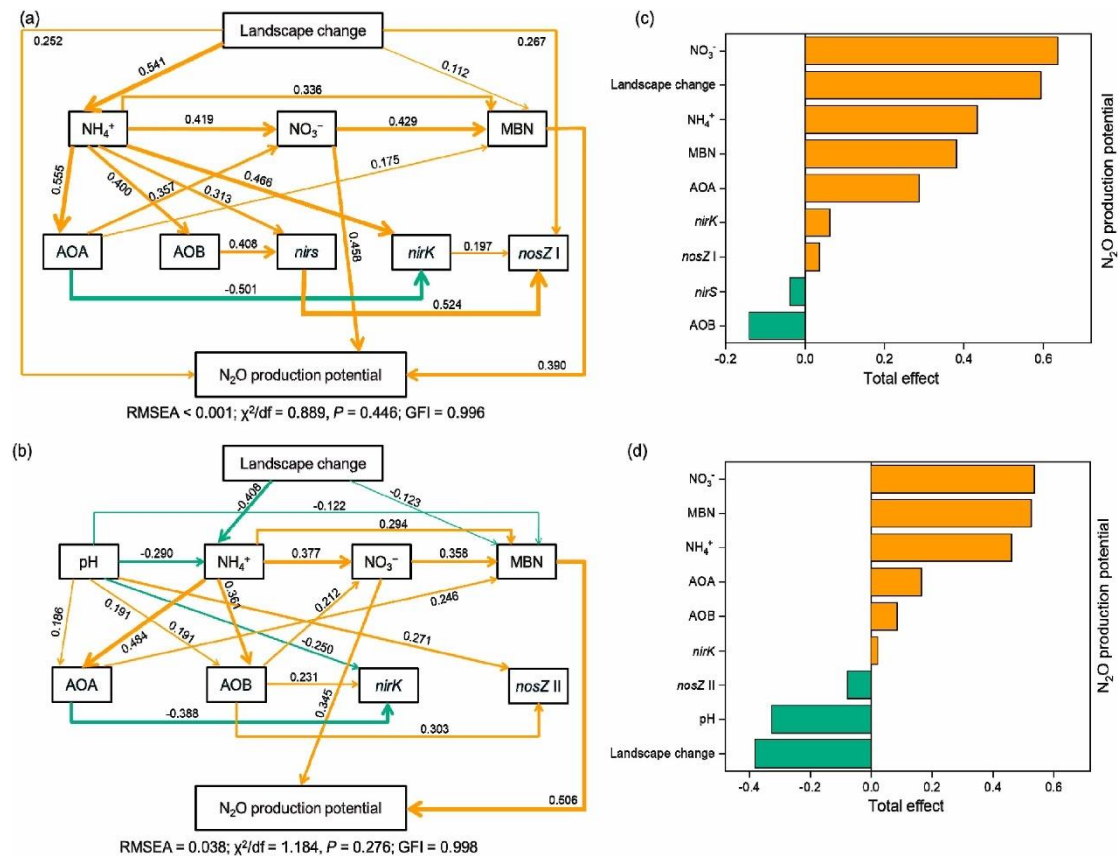


Fig. 6. Structural equation models (SEM) to evaluate the direct and indirect effects of landscape change, sediment properties and the abundance of functional genes on N_2O production potential under different habitat modification scenarios: (a) conversion of mudflats to *S. alterniflora* marshes; (b) conversion of *S. alterniflora* marshes to aquaculture ponds. Total standardized effects of multiple factors on N_2O production potential for the respective habitat modification scenarios are shown in panel (c) and (d).

4. Discussion

Large swaths of coastal mudflat in China have been transformed into marshes by the invasive *S. alterniflora* (Mao et al., 2019). To control the spread of *S. alterniflora* and boost food production, many of these marshes have been subsequently cleared and converted into aquaculture ponds (Duan et al., 2021). These drastic landscape transformations have been shown to alter the sediment organic carbon content, carbon remineralization and carbon GHG production (Yang et al., 2022). The rapid expansion of coastal aquaculture in China also raises the alarm of potential increase in N_2O production and emission, thanks to the increasing use of nitrogenous fertilizer and feeds in the farming process (Hu et al., 2012; Zhou et al., 2021).

Previous studies have shown that non-native plant species could increase N_2O emissions from coastal wetlands (Gao et al., 2019a, 2019c), likely by increasing organic input into the sediment (Wang et al., 2019a; Xia et al., 2021), which would promote microbial abundance

and nitrogen remineralization. This is supported by our observation of significantly higher sediment MBN, $\text{NH}_4^+\text{-N}$ and $\text{NO}_3^-\text{-N}$ concentrations in SAs relative to MFs (Fig. 2). An earlier meta-analysis has shown that increasing $\text{NH}_4^+\text{-N}$ availability can promote the growth of both AOA and AOB (Ouyang et al., 2018), which would lead to a higher N_2O production. Our correlation and SEM analyses indeed showed that both AOA *amoA* and AOB *amoA* abundances were positively correlated with sediment $\text{NH}_4^+\text{-N}$ concentrations (Fig. 6), and our incubation experiments also showed a significantly higher N_2O production potential in SAs than MFs (Fig. 4). These findings support our first hypothesis that conversion of MFs to SAs enhanced sediment N_2O production potential by increasing the supply of nitrogen substrates for microbial-mediated ammonia oxidation.

On the other hand, our data showed that the conversion of SAs to APs decreased sediment N_2O production potential (Fig. 4), which supported our second hypothesis. Some previous studies have also shown that conversion of coastal marshes to aquaculture ponds could reduce net N_2O emissions (Yang et al., 2017; Yuan et al., 2019; Tan et al., 2020). This at first glance is counter-intuitive, as the use of fertilizer and feeds in aquaculture is widely expected to increase N_2O production and emission (Hu et al., 2012; Williams and Crutzen, 2010). However, it is necessary to consider that some of the added nitrogen (as fertilizer or feeds) would have been sequestered into the sediment or harvested as biomass. Many of the coastal aquaculture ponds in China are for farming shrimp, which has a relatively high nutrient utilization efficiency and consequently, only a small percentage of the added nitrogen would be lost as N_2O emission (Yang et al., 2021). Meanwhile, the removal of *S. alterniflora* during the construction of aquaculture ponds would have eliminated plant-mediated supply of labile organics to the sediment, which may partly explain the lower $\text{NH}_4^+\text{-N}$ and $\text{NO}_3^-\text{-N}$ concentrations in AP sediment (Fig. 2). Furthermore, a common aquaculture management practice is to dry out the pond sediment and condition it by adding lime between farming seasons (Yang et al., 2021), which would have disrupted the sediment microbial community and its activity. These likely contributed to the lower sediment MBN and N_2O production potential relative to SAs (Fig. 2, Fig. 5).

Denitrification is a key process in N_2O dynamics in coastal and estuarine environments (Hou et al., 2015; Su et al., 2021, 2022). However, the functional genes for denitrification (i.e., *nirK*, *nirS*, *nosZ I* and *nosZ II*) were found to have limited influence on sediment N_2O production potential in this study (Fig. 6), which might be due to the overall low $\text{NO}_3^-\text{-N}$ concentrations across our study sites (Fig. 2) and that complete denitrification may produce N_2 instead of N_2O as the end-product (Ciarlo et al., 2008; Wilcock and Sorrell, 2008; Peralta et al., 2010). In contrast, N_2O production potential was most strongly correlated with the functional genes AOA *amoA* and AOB *amoA* (Fig. 5, Fig. 6), suggesting that ammonia oxidation was the overall rate-limiting step in N_2O production in these wetland ecosystems. This aligns with the findings of Bahram et al. (2022) that the abundance of AOA is a key factor determining the rate of N_2O emissions from global wetlands. Indeed, ammonia oxidizers can drive N_2O production (Hu et al., 2015) especially when $\text{NH}_4^+\text{-N}$ is the dominant form of available nitrogen (Lin et al., 2017; Wang et al., 2019b), such as the case in our study where sediment $\text{NH}_4^+\text{-N}$ concentration was an order of magnitude higher than $\text{NO}_3^-\text{-N}$ across all sampling sites (Fig. 2). It was also not surprising to find that AOA *amoA* was more abundant than AOB *amoA* (Fig. 3a and b), since AOA can better cope with stresses, giving them a competitive edge over AOB in hypoxic and hypersaline environment (Valentine, 2007; Sun et al., 2022), including wetlands (Sims et al., 2012; Wang et al., 2020; Lin et al., 2021).

5. Conclusions

This study investigated the effects of coastal habitat modification on sediment N_2O production potential across a broad geographical range in China. Our results suggest that conversion of mudflats to *S. alterniflora* marshes enhanced sediment N_2O production potential by increasing the supply of nitrogen substrates and the functional gene abundance for ammonia oxidation, whereas, contrary to common expectation, the subsequent conversion

of *S. alterniflora* marshes to aquaculture ponds reduced sediment N₂O production potential owing to a decrease in nitrogen substrate availability and AOA *amoA* gene abundance. These findings highlight that converting *S. alterniflora* marshes to aquaculture ponds could be an effective strategy to achieve multiple benefits of controlling an invasive species, boosting food production and decreasing sediment GHG emission. More importantly, using data from widely distributed sampling sites, we were able to derive common effect patterns of landscape transformation as the results of plant invasion and aquaculture reclamation across the broad geographical and climate range, from tropical to subtropical zones, regardless of local differences in hydrography, biodiversity, management practices or other variables. These findings will facilitate follow-on large-scale mapping and assessing landscape change effects on coastal ecosystems and N₂O emissions, for example, by incorporating GIS and remote sensing data. While we measured N₂O production in sediment, the actual emissions to the atmosphere could be further modulated by *in-situ* biological/abiotic factors. Measurements of *in-situ* N₂O emissions from the different habitats in future study, using methods such as flux chambers, will be valuable.

Author contribution statement

Conceptualization: Ping Yang, Kam W. Tang, Chuan Tong, Derrick Y. F. Lai, Yongxin Lin
Methodology: Ping Yang, Linhai Zhang, Xiao Lin, Yongxin Li, Manjing Ruan, Formal analysis: Ping Yang, Yan Hong, Lishan Tan, Derrick Y. F. Lai, Manjing Ruan, Validation: Ping Yang, Investigation: Ping Yang, Linhai Zhang, Xiao Lin, Yan Hong, Lishan Tan, Wanyi Zhu, Derrick Y. F. Lai, Data Curation: Ping Yang, Kam W. Tang, Chuan Tong, Writing-Original Draft: Ping Yang, Kam W. Tang. Writing - Review & Editing: Ping Yang, Kam W. Tang, Hong Yang, Derrick Y. F. Lai, Yongxin Li, Project Administration: Ping Yang, Chuan Tong, Hong Yang, Derrick Y. F. Lai, Funding acquisition: Ping Yang, Chuan Tong, Hong Yang, Derrick Y. F. Lai.

Acknowledgements

This research was supported by the Natural Science Foundation of Fujian Province, China (Grant No. 2020J01136, and 2022R1002006), the National Natural Science Foundation of China (NSFC) (Grant No. 41801070, and No. 41671088), and the Research Grants Council of the Hong Kong Special Administrative Region, China (Project No. CUHK 14122521).

References

- Bahram, M., Espenberg, M., Parn, J., Lehtovirta-Morley, L., Anslan, S., Kasak, K., Kõljalg, U., Liira, J., Maddison, M., Moora, M., Niinemets, Ü., Opik, M., Partel, M., Soosaar, K., Zobel, M., Hildebrand, F., Tedersoo, L., Mander, Ü., 2022. Structure and function of the soil microbiome underlying N₂O emissions from global wetlands. *Nat. Commun.* 13, 1430. <https://doi.org/10.1038/s41467-022-29161-3>.
- Batjes, N.H., 1996. Total carbon and nitrogen in the soils of the world. *Eur. J. Soil Sci.* 47, 151–163. <https://doi.org/10.1111/ejss.12115>.
- Butterbach-Bahl, K., Baggs, E.M., Dannenmann, M., Kiese, R., Zechmeister-Boltenstern, S., 2013. Nitrous oxide emissions from soils: how well do we understand the processes and their controls? *Philos. T. R. Soc. B: Biol. Sci.* 368, 20130122. <https://doi.org/10.1098/rstb.2013.0122>.

- Chen, B.B., Sun, Z.G., 2020. Effects of nitrogen enrichment on variations of sulfur in plant-soil system of *Suaeda salsa* in coastal marsh of the Yellow River estuary. *China. Ecol. Indic.* 109, 105797 <https://doi.org/10.1016/j.ecolind.2019.105797>.
- Chmura, G.L., Anisfeld, S.C., Cahoon, D.R., Lynch, J.C., 2003. Global carbon sequestration in tidal, saline wetland soils. *Global Biogeochem. Cycles* 17 (4), 1111. <https://doi.org/10.1029/2002GB001917>.
- Ciarlo, E., Conti, M., Bartoloni, N., Rubio, G., 2008. Soil N₂O emissions and N₂O/(N₂O+ N₂) ratio as affected by different fertilization practices and soil moisture. *Biol. Fertil. Soils* 44, 991–995. <https://doi.org/10.1007/s00374-008-0302-6>.
- Duan, Y.Q., Li, X., Zhang, L.P., Chen, D., Liu, S.A., Ji, H.Y., 2020. Mapping national-scale aquaculture ponds based on the Google Earth Engine in the Chinese coastal zone. *Aquaculture* 520, 734666. <https://doi.org/10.1016/j.aquaculture.2019.734666>.
- Duan, Y.Q., Tian, B., Li, X., Liu, D.Y., Sengupta, D., Wang, Y.J., Peng, Y., 2021. Tracking changes in aquaculture ponds on the China coast using 30 years of Landsat images. *Int. J. Appl. Earth Obs.* 102, 102383.
- Gao, D.Z., Hou, L.J., Liu, M., Zheng, Y.L., Yin, G.Y., Niu, Y.H., 2021. N₂O emission dynamics along an intertidal elevation gradient in a subtropical estuary: importance of N₂O consumption. *Environ. Res.* 205, 112432 <https://doi.org/10.1016/j.envres.2021.112432>.
- Gao, G.F., Li, P.F., Zhong, J.X., Shen, Z.J., Chen, J., Li, Y.T., Isabwe, A., Zhu, X.Y., Ding, Q.S., Zhang, S., Gao, C.H., Zheng, H.L., 2019a. *Spartina alterniflora* invasion alters soil bacterial communities and enhances soil N₂O emissions by stimulating soil denitrification in mangrove wetland. *Sci. Total Environ.* 653, 231–240. <https://doi.org/10.1016/j.scitotenv.2018.10.277>.
- Gao, D.Z., Liu, M., Hou, L.J., Lai, D.Y.F., Wang, W.Q., Li, X.F., Zeng, A.Y., Zheng, Y.L., Han, P., Yang, Y., Yin, G.Y., 2019b. Effects of shrimp-aquaculture reclamation on sediment nitrate dissimilatory reduction processes in a coastal wetland of southeastern China. *Environ. Pollut.* 255, 113219 <https://doi.org/10.1016/j.envpol.2019.113219>.
- Gao, D.Z., Hou, L.J., Li, X.F., Liu, M., Zheng, Y.L., Yin, G.Y., Yang, Y., Liu, C., Han, P., 2019c. Exotic *Spartina alterniflora* invasion alters soil nitrous oxide emission dynamics in a coastal wetland of China. *Plant Soil* 442, 233–246. <https://doi.org/10.1007/s11104-019-04179-7>.
- He, G.S., Wang, K.Y., Zhong, Q.C., Zhang, G.L., van den Bosch, C.K., Wang, J.T., 2021. Agroforestry reclamations decreased the CO₂ budget of a coastal wetland in the Yangtze estuary. *Agric. For. Meteorol.* 296, 108212 <https://doi.org/10.1016/j.agrformet.2020.108212>.
- Hellman, M., Bonilla-Rosso, G., Widerlund, A., Juhanson, J., Hallin, S., 2019. External carbon addition for enhancing denitrification modifies bacterial community composition and affects CH₄ and N₂O production in sub-arctic mining pond sediments. *Water Res.* 158, 22–33. <https://doi.org/10.1016/j.watres.2019.04.007>.
- Hou, L.J., Yin, G.Y., Liu, M., Zhou, J.L., Zheng, Y.L., Gao, J., Zong, H.B., Yang, Y., Gao, L., Tong, C.F., 2015. Effects of sulfamethazine on denitrification and the associated N₂O release in estuarine and coastal sediments. *Environ. Sci. Technol.* 49 (1), 326–333. <https://doi.org/10.1021/es504433r>.
- Hu, H.W., Chen, D., He, J.Z., 2015. Microbial regulation of terrestrial nitrous oxide formation: understanding the biological pathways for prediction of emission rates. *FEMS Microbiol. Rev.* 39, 729–749. <https://doi.org/10.1093/femsre/fuv021>. 8

- Hu, Z., Lee, J.W., Chandran, K., Kim, S., Khanal, S.K., 2012. Nitrous oxide (N₂O) emission from aquaculture: a review. *Environ. Sci. Technol.* 46 (12), 6470–6480.
- IPCC, 2019. In: Calvo Buendia, E., Tanabe, K., Kranjc, A., Baasansuren, J., Fukuda, M., Ngarize, S. (Eds.), 2019 Refinement to the 2006 IPCC Guidelines for National Greenhouse Gas Inventories, Volum 4. IPCC. Kanagawa, Switzerland. Japan (Chapter 07).
- Jia, M.M., Wang, Z.M., Mao, D.H., Ren, C.Y., Wang, C., Wang, Y.Q., 2021. Rapid, robust, and automated mapping of tidal flats in China using time series Sentinel-2 images and Google Earth Engine. *Remote Sens. Environ.* 255, 112285 <https://doi.org/10.1016/j.rse.2021.112285>.
- Lin, Y.X., Ding, W.X., Liu, D.Y., He, T.H., Yoo, G., Yuan, J.J., Chen, Z.M., Fan, J.L., 2017. Wheat straw-derived biochar amendment stimulated N₂O emissions from rice paddy soils by regulating the amoA genes of ammonia-oxidizing bacteria. *Soil Biol. Biochem.* 113, 89–98. <https://doi.org/10.1016/j.watres.2021.117682>.
- Lin, Y.X., Hu, H.W., Ye, G.P., Fan, J.B., Ding, W.X., He, Z.Y., Zheng, Y., He, J.Z., 2021. Ammonia-oxidizing bacteria play an important role in nitrification of acidic soils: a meta-analysis. *Geoderma* 404, 115395. <https://doi.org/10.1016/j.geoderma.2021.115395>.
- Liu, J.G., Hartmann, S.C., Keppler, F., Lai, D.Y.F., 2019. Simultaneous abiotic production of greenhouse gases (CO₂, CH₄, and N₂O) in Subtropical Soils. *J. Geophys. Res.- Biogeo.* 124 (7), 1977–1987. <https://doi.org/10.1029/2019JG005154>.
- Liu, M.Y., Mao, D.H., Wang, Z.M., Li, L., Man, W.D., Jia, M.M., Ren, C.Y., Zhang, Y.Z., 2018. Rapid invasion of *Spartina alterniflora* in the coastal zone of mainland China: new observations from Landsat OLI images. *Rem. Sens.* 10, 1933. <https://doi.org/10.3390/rs10121933>.
- Mao, D.H., Liu, M.Y., Wang, Z.M., Li, L., Man, W.D., Jia, M.M., Zhang, Y., 2019. Rapid invasion of *Spartina alterniflora* in the coastal zone of mainland China: spatiotemporal patterns and human prevention. *Sensors* 19 (10), 2308. <https://doi.org/10.3390/s19102308>.
- Murray, N.J., Phinn, S.R., DeWitt, M., Ferrari, R., Johnston, R., Lyons, M.B., Fuller, R.A., 2019. The global distribution and trajectory of tidal flats. *Nature* 565, 222–225. <https://doi.org/10.1038/s41586-018-0805-8>.
- Ouyang, Y., Evans, S.E., Friesen, M.L., Tiemann, L.K., 2018. Effect of nitrogen fertilization on the abundance of nitrogen cycling genes in agricultural soils: a metaanalysis of field studies. *Soil Biol. Biochem.* 127, 71–78. <https://doi.org/10.1016/j.soilbio.2018.08.024>.
- Peralta, A.L., Matthews, J.W., Kent, A.D., 2010. Microbial community structure and denitrification in a wetland mitigation bank. *Appl. Environ. Microbiol.* 76, 4207–4215. <https://doi.org/10.1128/aem.02977-09>.
- Ren, C.Y., Wang, Z.M., Zhang, Y.Z., Zhang, B., Chen, L., Xia, Y.B., Xiao, X.M., Doughty, R. B., Liu, M.Y., Jia, M., Mao, D.H., Song, K.S., 2019. Rapid expansion of coastal aquaculture ponds in China from Landsat observations during 1984–2016. *J. Appl. Earth Obs.* 82, 101902 <https://doi.org/10.1016/j.jag.2019.101902>.
- Sims, A., Horton, J., Gajaraj, S., McIntosh, S., Miles, R.J., Mueller, R., Reed, R., Hu, Z., 2012. Temporal and spatial distributions of ammonia-oxidizing archaea and bacteria and their ratio as an indicator of oligotrophic conditions in natural wetlands. *Water Res.* 46, 4121–4129. <https://doi.org/10.1016/j.watres.2012.05.007>.
- Su, X.X., Wen, T., Wang, Y.M., Xu, J.S., Cui, L., Zhang, J.B., Xue, X.M., Ding, K., Tang, Y. J., Zhu, Y.G., 2021. Stimulation of N₂O emission via bacterial denitrification driven by

- acidification in estuarine sediments. *Global Change Biol.* 27, 5564–5579. <https://doi.org/10.1111/gcb.15863>.
- Su, X.X., Yang, L.Y., Yang, K., Tang, Y.J., Wen, T., Wang, Y.M., Rillig, M.C., Rohe, L., Pan, J.L., Li, H., Zhu, Y.G., 2022. Estuarine plastisphere as an overlooked source of N₂O production. *Nat. Commun.* 13, 3884. <https://doi.org/10.1038/s41467-022-31584-x>.
- Sun, X.X., Zhao, J., Zhou, X., Bei, Q.C., Xia, W.W., Zhao, B.Z., Zhang, J.B., Jia, Z.J., 2022. Salt tolerance-based niche differentiation of soil ammonia oxidizers. *ISME J.* 16, 412–422. <https://doi.org/10.1038/s41396-021-01079-6>.
- Sun, Z.G., Sun, W.G., Tong, C., Zeng, C.S., Yu, X., Mou, X.J., 2015. China's coastal wetlands: conservation history, implementation efforts, existing issues and strategies for future improvement. *Environ. Int.* 79, 25–41. <https://doi.org/10.1016/j.envint.2015.02.017V>.
- Tian, H.Q., Xu, R.T., Canadell, J.G., Thompson, R.L., Winiwarter, W., Suntharalingam, P., Davidson, E.A., Ciais, P., Jackson, R.B., et al., 2020. A comprehensive quantification of global nitrous oxide sources and sinks. *Nature* 586, 248–256. <https://doi.org/10.1038/s41586-020-2780-0>.
- Tan, L.S., Ge, Z.M., Ji, Y.H., Lai, D.Y.F., Temmerman, S., Li, S.H., Li, X.Z., Tang, J.W., 2022. Land use and land cover changes in coastal and inland wetlands cause soil carbon and nitrogen loss. *Global Ecol. Biogeogr.* 31 (12), 2541–2563. <https://doi.org/10.1111/geb.13597>.
- Tan, L.S., Ge, Z.M., Zhou, X.H., Li, S.H., Li, X.Z., Tang, J.W., 2020. Conversion of coastal wetlands, riparian wetlands, and peatlands increases greenhouse gas emissions: a global meta-analysis. *Global Change Biol.* 26, 1638–1653. <https://doi.org/10.1111/gcb.14933>.
- Templer, P., Findlay, S., Lovett, G., 2003. Soil microbial biomass and nitrogen transformations among five tree species of the Catskill Mountains, New York, USA. *Soil Biol. Biochem.* 35 (4), 607–613. [https://doi.org/10.1016/s0038-0717\(03\)00006-3](https://doi.org/10.1016/s0038-0717(03)00006-3).
- Toyoda, S., Yano, M., Nishimura, S.I., Akiyama, H., Hayakawa, A., Koba, K., Ogawa, N. O., 2011. Characterization and production and consumption processes of N₂O emitted from temperate agricultural soils determined via isotopomer ratio analysis. *Global Biogeochem. Cycles* 25, 96–101. <https://doi.org/10.1029/2009GB003769>.
- Valentine, D.L., 2007. Adaptations to energy stress dictate the ecology and evolution of the Archaea. *Nat. Rev. Microbiol.* 5, 316–323. <https://doi.org/10.1038/nrmicro1619>.
- Walker, L.R., Smith, S.D., 1992. Impacts of invasive plants on community and ecosystem properties. In: Luken, J.O., Thieret, J.W. (Eds.), *Assessment and Management of Plant Invasion*. Springer-Verlag, New York, pp. 69–94.
- Wang, C., Tang, S.Y., He, X.J., Ji, G.D., 2020. The abundance and community structure of active ammonia-oxidizing archaea and ammonia-oxidizing bacteria shape their activities and contributions in coastal wetlands. *Water Res.* 171, 115464 <https://doi.org/10.1016/j.watres.2019.115464>.
- Wang, W.Q., Sardans, J., Wang, C., Zeng, C.S., Tong, C., Chen, G., Huang, J.F., Pan, H.R., Peguero, G., Vallicrosa, H., Penuelas, J., 2019a. The response of stocks of C, N, and P to plant invasion in the coastal wetlands of China. *Global Change Biol.* 25, 733–743. <https://doi.org/10.1111/gcb.14491>.
- Wang, L., Li, K., Sheng, R., Li, Z.H., Wei, W.X., 2019b. Remarkable N₂O emissions by draining fallow paddy soil and close link to the ammonium-oxidizing archaea communities. *Sci. Rep.* 9, 2550. <https://doi.org/10.1038/s41598-019-39465-y>.

- Wang, W.Q., Sardans, J., Wang, C., Zeng, C.S., Tong, C., Asensio, D., Peñuelas, J., 2017. Relationships between the potential production of the greenhouse gases CO₂, CH₄ and N₂O and soil concentrations of C, N and P across 26 paddy fields in southeastern China. *Atmos. Environ.* 164, 458–467. <https://doi.org/10.1016/j.atmosenv.2017.06.023>.
- Wilcock, R.J., Sorrell, B.K., 2008. Emissions of greenhouse gases CH₄ and N₂O from lowgradient streams in agriculturally developed catchments. *Water Air Soil Pollut.* 188, 155–170. <https://doi.org/10.1029/2017gb005826>.
- Williams, J., Crutzen, P.J., 2010. Nitrous oxide from aquaculture. *Nat. Geosci.* 3 (3), 143. <https://doi.org/10.1038/ngeo804>, 143.
- World Meteorological Organization, 2021. WMO Greenhouse Gas Bulletin (GHG Bulletin) - No.17: the State of Greenhouse Gases in the Atmosphere Based on Global Observations through 2020.
- Wu, D., Well, R., Cardenas, L.M., Fuß, R., Lewicka-Szczebak, D., Köster, J.R., Brüggemann, N., Bol, R., 2019. Quantifying N₂O reduction to N₂ during denitrification in soils via isotopic mapping approach: model evaluation and uncertainty analysis. *Environ. Res.* 179, 108806 <https://doi.org/10.1016/j.envres.2019.108806>.
- Xia, S.P., Wang, W.Q., Song, Z.L., Kuzyakov, Y., Guo, L.D., Van Zwieten, L., Li, Q., Hartley, I.P., Yang, Y.H., Wang, Y.D., Quine, T.A., Liu, C.Q., Wang, H.L., 2021. *Spartina alterniflora* invasion controls organic carbon stocks in coastal marsh and mangrove soils across tropics and subtropics. *Global Change Biol.* 27, 1627–1644. <https://doi.org/10.1111/gcb.15516>.
- Xu, L., He, N.P., Yu, G.R., 2020. Nitrogen storage in China's terrestrial ecosystems. *Sci. Total Environ.* 709, 136201 <https://doi.org/10.1016/j.scitotenv.2019.136201>.
- Yang, P., Bastviken, D., Jin, B.S., Mou, X.J., Tong, C., 2017. Effects of coastal marsh conversion to shrimp aquaculture ponds on CH₄ and N₂O emissions. *Estuar. Coast Shelf Sci.* 199, 125–131. <https://doi.org/10.1016/j.ecss.2017.09.023>.
- Yang, P., Zhao, G., Tong, C., Tang, K.W., Lai, D.Y.F., Li, L., Tong, C., 2021. Assessing nutrient budgets and environmental impacts of coastal land-based aquaculture system in southeastern China. *Agric. Ecosyst. Environ.* 322, 107662 <https://doi.org/10.1016/j.agee.2021.107662>.
- Yang, P., Zhang, L.H., Lai, D.Y.F., Yang, H., Tan, L.S., Luo, L.J., Tong, C., Hong, Y., Zhu, W.Y., Tang, K.W., 2022. Landscape change affects soil organic carbon mineralization and greenhouse gas production in coastal wetlands. *Global Biogeochem. Cycles* 36, e2022GB007469. <https://doi.org/10.1029/2022GB007469>.
- Yang, W., An, S.Q., Zhao, H., Xu, L.Q., Qiao, Y.J., Cheng, X.L., 2016. Impacts of *Spartina alterniflora* invasion on soil organic carbon and nitrogen pools sizes, stability, and turnover in a coastal salt marsh of eastern China. *Ecol. Eng.* 86, 174–182. <https://doi.org/10.1016/j.ecoleng.2015.11.010>.
- Yin, G.Y., Hou, L.J., Liu, M., Li, X.F., Zheng, Y.L., Gao, J., Lin, X.B., 2017. DNRA in intertidal sediments of the Yangtze Estuary. *J. Geophys. Res.-Biogeo.* 122 (8), 1988–1998. <https://doi.org/10.1002/2017JG003766>.
- Yuan, J.J., Xiang, J., Liu, D.Y., Kang, H., He, T.H., Kim, S., Lin, Y.X., Freeman, C., Ding, W.X., 2019. Rapid growth in greenhouse gas emissions from the adoption of industrial-scale aquaculture. *Nat. Clim. Change* 9 (4), 318–322. <https://doi.org/10.1038/s41558-019-0425-9>.

Zhang, Y.H., Xu, X.J., Li, Y., Huang, L.D., Xie, X.J., Dong, J.M., Yang, S.Q., 2016. Effects of *Spartina alterniflora* invasion and exogenous nitrogen on soil nitrogen mineralization in the coastal salt marshes. *Ecol. Eng.* 87, 281–287. <https://doi.org/10.1016/j.ecoleng.2015.12.003>.

Zhou, Y., Huang, M., Tian, H.Q., Xu, R.T., Ge, J., Yang, X.G., Liu, R.X., Sun, Y.X., Pan, S. F., Gao, Q.F., Dong, S.L., 2021. Four decades of nitrous oxide emission from Chinese aquaculture underscores the urgency and opportunity for climate change mitigation. *Environ. Res. Lett.* 16 (11), 114038 <https://doi.org/10.1088/1748-9326/ac3177>.